RSC Advances

ROYAL SOCIETY OF CHEMISTRY

www.rsc.org/advances

Journal Name

ARTICLE

Type-I Clathrates of $K_{7.69(2)}Cu_{2.94(6)}Ge_{43.06(6)}$ and $Rb_8Ag_{2.79(4)}Ge_{43.21(4)}$

Hui Zhang,[a] Xuguang Xu,[b] Wei Li,[b] Gang Mu,[b] Fu-Qiang Huang,[a,c†] and Xiao-Ming Xie[b]

Received 00th January 20xx,
Accepted 00th January 20xx

DOI: 10.1039/x0xx00000x

www.rsc.org/

Type-I clathrates of $K_{7.69(2)}Cu_{2.94(6)}Ge_{43.06(6)}$ and $Rb_8Ag_{2.79(4)}Ge_{43.21(4)}$ are synthesized directly from corresponding elements. The structures are resolved by powder XRD data by means of a least-squares technique using WinCSD program. The refined lattice parameters are a = 10.70783(3) Å and a = 10.84493(3) Å for $K_{7.69(2)}Cu_{2.94(6)}Ge_{43.06(6)}$ and $Rb_8Ag_{2.79(4)}Ge_{43.21(4)}$, respectively. The electronic band structure and density of states indicate $K_8Cu_3Ge_{43}$ and $Rb_8Ag_3Ge_{43}$ are *p*-type semiconductors with narrow indirect band gaps of 0.33 and 0.24 eV. In addition, $K_{7.69(2)}Cu_{2.94(6)}Ge_{43.06(6)}$ displays a diamagnetism with χ = -1.102(1)×10^{-3} emu·mol^{-1} in the field of 7 T at 400 K and has a strong Einstein model with θ_E = 56.3(1) K and θ_D = 297(3) K.

Introduction

Clathrate compounds comprise host frameworks that embrace guest species in polyhedral cages.[1] Inorganic clathrates form some structure types according to respective polyhedral types and their arrangements: such as type-I clathrates,[1-3] type-II clathrates,[4-5] type-III clathrate,[6] type-VIII clathrates,[7-8] type-IX clathrate,[9] type-X clathrates,[10] *etc*. Clathrates can be classified into cationic[1-4,7-9], neutral[5]and anionic[6,10] according to the charge distribution between framework and guest atoms, as well as clathrate hydrates of natural gases.[11] The recent impetuous interest in clathrates of tetrels (elements of group 14) in which the host framework is based on Si, Ge, or Sn atoms is motivated in particular by the search for a new generation of efficient thermoelectric materials.[12]

The Zintl-Klemm rule offers an explanation for the formation of electronically-balanced clathrates with partial substitutions on the framework and guest atom sites.[3,6] The recent growing interest in clathrates of tetrels (elements of group 14) in which the host framework is based on Si, Ge, or Sn atoms is motivated in particular by the search for a new generation of efficient thermoelectric materials.[12] The most anionic 14 group element M (M = Si/Ge/Sn) based type-I clathrates with alkaline metal A (A = Na, K, Rb, Cs) in the cages are built with 13 group elements T (T = B, Al, Ga, In): such as Ge based clathrates $K_7B_7Ge_{39}$,[3] $K_8Al_8Ge_{38}$,[13] $K_8Al_{23.3}Ge_{22.7}$,[14] $K_8Ga_{23}Ge_{23}$,[14-15] $K_8In_6Ge_{40}$,[16] $K_8In_{8.14}Ge_{37.86}$,[17] $K_8In_{16}Ge_{30}$,[15] $Rb_8Al_{7.84}Ge_{38.16}$,[18] $Rb_8Ga_8Ge_{38}$,[19] $Rb_8In_{7.81}Ge_{38.19}$,[17] etc. There are only a few transition metal clathrates: e.g. $K_8Hg_{3.19}Ge_{42.81}$,[20] $Rb_8Hg_{3.03}Ge_{42.97}$,[20] and (Rb, K)$_{8-x}$Au$_y$Ge$_{46-y}$.[21] We found alkaline earth metal and transition metal clathrate of $Ba_8Au_{5.3}Ge_{43.7}$ has good thermoelectric properties with ZT=0.3~0.9.[22] It is worth to explore alkali metal and transition metal clathrates for potential thermoelectric applications.

Herein the synthesis and structure of $K_{7.69(2)}Cu_{2.94(6)}Ge_{43.06(6)}$ and $Rb_8Ag_{2.79(4)}Ge_{43.21(4)}$ are investigated. The magnetic properties and heat capacity of $K_{7.69(2)}Cu_{2.94(6)}Ge_{43.06(6)}$ are also presented.

Results and discussion

The synthesized $K_{7.69(2)}Cu_{2.94(6)}Ge_{43.06(6)}$ and $Rb_8Ag_{2.79(4)}Ge_{43.21(4)}$ products are grey blocks. The element compositions of $K_{8.6(1)}Cu_{2.8(1)}Ge_{43.2(1)}$ and $Rb_{9(2)}Ag_{2.2(5)}Ge_{43.8(5)}$ are confirmed by EDX analysis. Composition and occupancy of $K_{7.69(2)}Cu_{2.94(6)}Ge_{43.06(6)}$ and $Rb_8Ag_{2.79(4)}Ge_{43.21(4)}$ are further refined by powder XRD data using *WinCSD* program.[23]

The systematic absences are same (hhl: 2h+l=2n and h00: h=2n) for $Pm\bar{3}n$(223) and $P\bar{4}3n$(218) space groups. Transition metal with a low amount of substitution in type-I clathrates[20-22] usually locate at 6c site like most anionic type-I clathrates with group 13 elements (B/Al/Ga/In) in $Pm\bar{3}n$ space group.[1-3, 13-19] Only a few cationic type-I clathrates $Ge_{38}P_8I_8$[24], $Ge_{38}As_8I_8$[24], $Ge_{38}Te_{16}$[25], etc. crystallize in $P\bar{4}3n$(218) space group in which double 8e sites replace 16i site in $Pm\bar{3}n$. For $K_{7.69(2)}Cu_{2.94(6)}Ge_{43.06(6)}$ and $Rb_8Ag_{2.79(4)}Ge_{43.21(4)}$ with low amount of Cu and Ag substitution for Ge we choose cubic $P\bar{4}3n$(223) space group.

During the initial steps of the refinement, all framework atoms are treated as Ge, and the guest atoms at 2*a* sites (K1/Rb1) and 6*d* sites (K2/Rb2) in cubic $Pm\bar{3}n$ (223) space group. Subsequent refinement sets Cu1/Ag1 at 6*c* position with Ge1

[a] *CAS Key Laboratory of Materials for Energy Conversion and State Key Laboratory of High Performance Ceramics and Superfine Microstructures, Shanghai Institute of Ceramics, Chinese Academy of Sciences, Shanghai 200050, P. R. China.*
[b] *State Key Laboratory of Functional Materials for Informatics and Shanghai Center for Superconductivity, Shanghai Institute of Microsystem and Information Technology, Chinese Academy of Sciences, Shanghai 200050, P. R. China.*
[c] *Beijing National Laboratory for Molecular Sciences, College of Chemistry and Molecular Engineering, Peking University, Beijing 100871, P. R. China.*
† Email:huangfq@mail.sic.ac.cn. Tel: 86-21-52411620
Electronic Supplementary Information (ESI) available: CCDC-1401202-1401203. See DOI: 10.1039/x0xx00000x

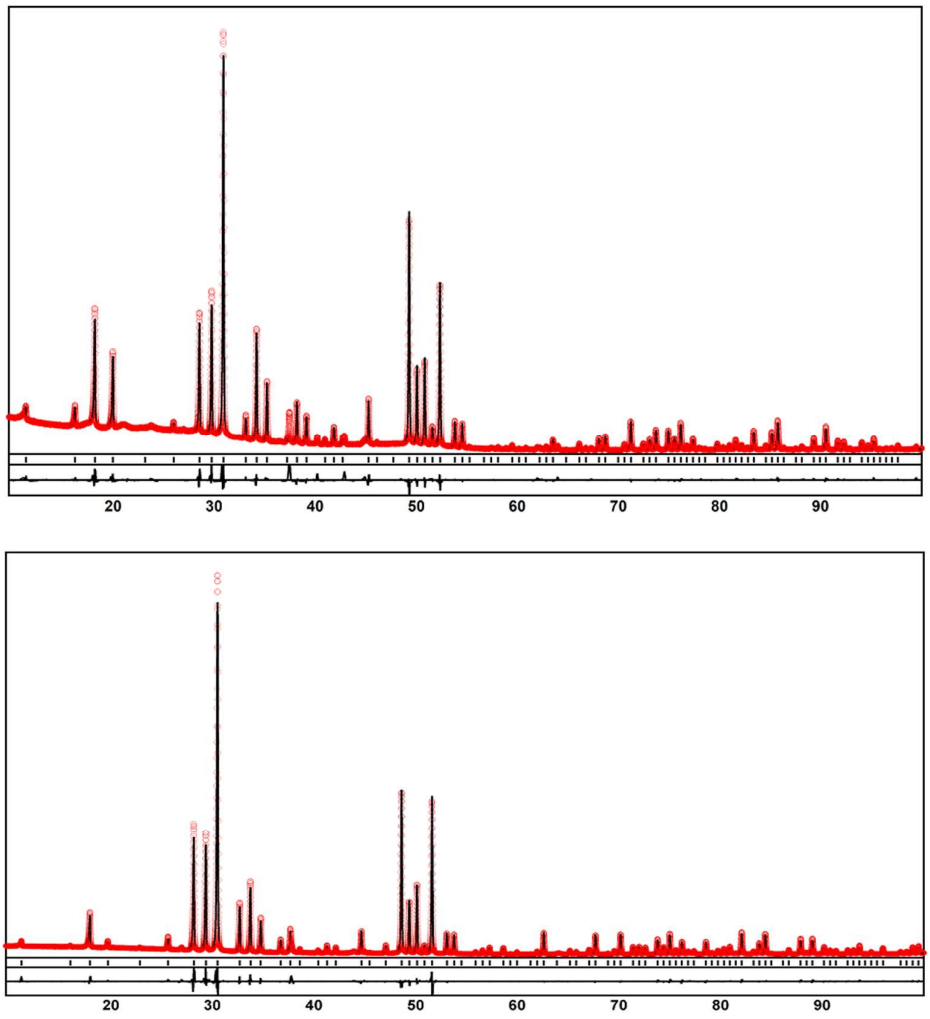

Figure 1. Refined XRD patterns of $K_{7.69(2)}Cu_{2.94(6)}Ge_{43.06(6)}$ (top) and $Rb_8Ag_{2.79(4)}Ge_{43.21(4)}$ (bottom)

Table 1. Fractional atomic coordinates, isotropic or equivalent isotropic displacement parameters (Å^2) and occupancy for $K_{7.69(2)}Cu_{2.94(6)}Ge_{43.06(6)}$ and $Rb_8Ag_{2.79(4)}Ge_{43.21(4)}$ in cubic $Pm\bar{3}n$ (223) space group.

Label	Sites	x	y	z	B_{iso}/B_{equ}	Occ.
$K_{7.69(2)}Cu_{2.94(6)}Ge_{43.06(6)}$, a = 10.70783(3) Å, R = 5.78%						
K1	2a	0	0	0	0.277(2)	1
K2	24k	0.2598(6)	0.4723(4)	0	0.341 (2)	0.237(1)
Ge1/Cu1	6c	1/4	0	1/2	1.330(2)	0.51(1)/0.49
Ge2	16i	0.18308(4)	x	x	0.933(2)	1
Ge3	24k	0	0.31124(5)	0.11862(5)	0.956(2)	1
$Rb_8Ag_{2.79(4)}Ge_{43.21(4)}$, a = 10.84493(3) Å, R = 5.36%						
Rb1	2a	0	0	0	1.105(2)	1
Rb2	6d	1/4	1/2	0	2.142(2)	1
Ge1/Ag1	6c	1/4	0	1/2	1.495(2)	0.535(6)/0.465
Ge2	16i	0.18323(5)	x	x	0.984(2)	1
Ge3	24k	0	0.30716(6)	0.11855(6)	0.876(2)	1

Table 2. Selected geometric parameters (Å, °) for $K_{7.69(2)}Cu_{2.94(6)}Ge_{43.06(6)}$ and $Rb_8Ag_{2.79(4)}Ge_{43.21}$ in cubic $Pm\bar{3}n$ (223) space group.

$K_{7.69(2)}Cu_{2.94(6)}Ge_{43.06(6)}$					
K1—8Ge2	3.3955 (5)	K2—2Ge1	3.872 (5)	Ge3—2Ge2	2.4906 (6)
K1—12Ge3	3.5667 (6)	K2—1Ge1	3.931 (5)	Ge3—1Ge3	2.5404 (8)
K2—2Ge3	3.413 (5)	K2—2Ge2	4.121 (2)	Ge3—Ge1—Ge3	109.05 (2)
K2—1Ge1	3.504 (5)	K2—2Ge3	4.165 (1)	Ge3—Ge1—Ge3	110.32 (2)
K2—2Ge3	3.511 (5)	K2—2Ge2	4.258 (4)	Ge3—Ge2—Ge2	107.24 (3)
K2—2Ge3	3.627 (5)	K2—1Ge3	4.414 (4)	Ge3—Ge2—Ge3	111.61 (3)
K2—2Ge2	3.757 (4)	Ge1—4Ge3	2.4625 (6)	Ge2—Ge3—Ge2	103.83 (3)
K2—1Ge3	3.827 (4)	Ge2—1Ge2	2.4822 (7)	Ge1—Ge3—Ge2	107.10 (2)
K2—2Ge2	3.829 (2)	Ge2—3Ge3	2.4906 (6)	Ge2—Ge3—Ge3	106.09 (3)
K2—2Ge3	3.837 (5)	Ge3—1Ge1	2.4625 (6)	Ge1—Ge3—Ge3	124.84 (3)
$Rb_8Ag_{2.79(4)}Ge_{43.21}$					
Rb1—8Ge2	3.4417 (6)	Ge2—1Ge2	2.5086 (8)	Ge3—Ge2—Ge2	108.09 (3)
Rb1—12Ge3	3.5705 (7)	Ge2—3Ge3	2.4993 (7)	Ge3—Ge2—Ge3	110.81 (3)
Rb2—8Ge3	3.6576 (5)	Ge3—1Ge1	2.5311 (7)	Ge2—Ge3—Ge2	105.32 (3)
Rb2—4Ge1	3.8343 (1)	Ge3—2Ge2	2.4993 (7)	Ge1—Ge3—Ge2	106.63 (3)
Rb2—8Ge2	4.0342 (1)	Ge3—1Ge3	2.571 (1)	Ge2—Ge3—Ge3	106.30 (3)
Rb2—4Ge3	4.1830 (7)	Ge3—Ge1—Ge3	108.50 (2)	Ge1—Ge3—Ge3	124.28 (3)
Ge1—4Ge3	2.5311 (7)	Ge3—Ge1—Ge3	111.44 (2)		

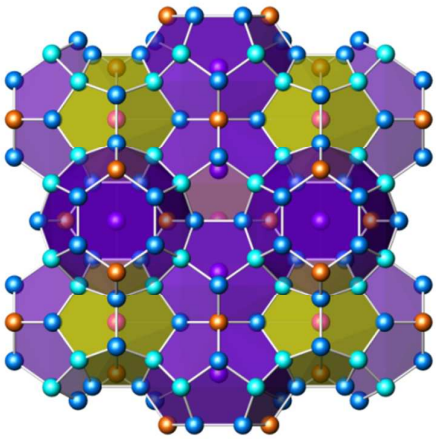

Figure 2. Crystal structures of $Rb_8Ag_{2.79(4)}Ge_{43.21(4)}$: brown Ge1 at 6*c* sites, cyan Ge2 at 16*i* and blue Ge3 at 24*k* sites form the tetrakaidecahedra caged with violet Rb2, Ge2 and Ge3 construct pentagonal dodecahedra caged with pink Rb1.

atoms. The isotropic atomic displacement parameters for K2 are large. Further refinement allowed the site position of K2shift from 6*d* sites (1/4, 0, 1/2) to 24*k* sites (*x*, 0, *y*) and the refined occupancy is 0.237(1). The K vacancy is common in K content clathrates $K_{6.71}Au_{2.21}Ge_{43.79}$.[21] For Rb2 neither split model nor partial occupancy reduces the displacement parameters. The refined XRD patterns for $K_{7.69(2)}Cu_{2.94(6)}Ge_{43.06(6)}$ and $Rb_8Ag_{2.83(2)}Ge_{43.17(2)}$ with *R* = 5.78% and *R* = 5.36% are given in (figure 1). The final atomic coordinates, site occupancies, isotropic atomic displacement parameters and *R* factors for $K_{7.69(2)}Cu_{2.94(6)}Ge_{43.06(6)}$ and $Rb_8Ag_{2.79(4)}Ge_{43.21(4)}$ are listed in table 1. The important interatomic distances of $K_{7.69(2)}Cu_{2.94(6)}Ge_{43.06(6)}$ and $Rb_8Ag_{2.79(4)}Ge_{43.21(4)}$ are given in

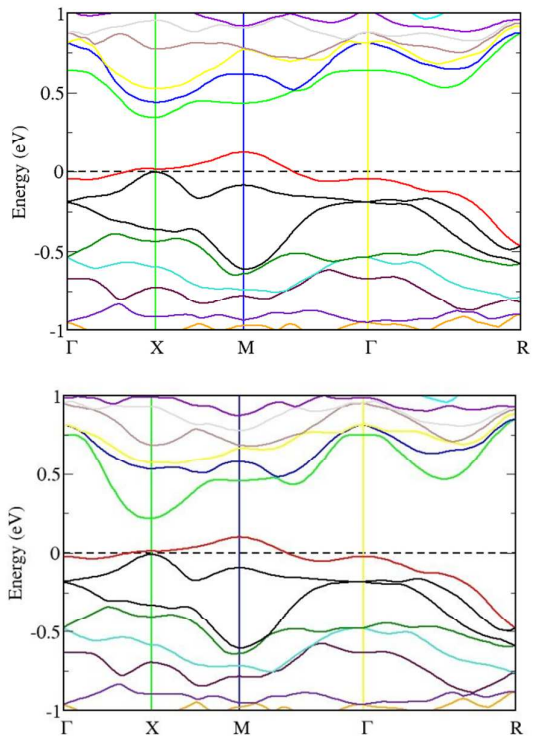

Figure 3. The energy band structure of (top) $K_8Cu_3Ge_{43}$ and (bottom) $Rb_8Ag_3Ge_{43}$ displaying an indirect *p*-type semiconductor with energy band gap of 0.33 and 0.24 eV, respectively.

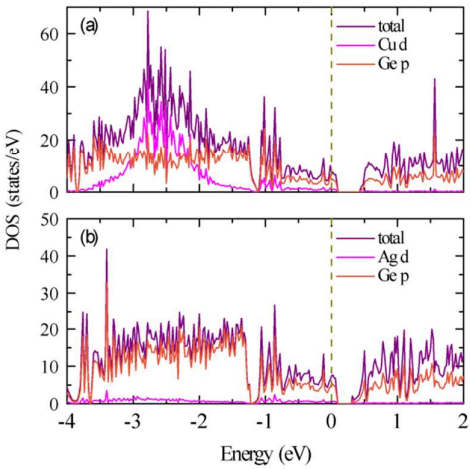

Figure 4. Total and partial density of states of Cu *d*, Ag *d*, Ge *p* states for (a) $K_8Cu_3Ge_{43}$ and (b) $Rb_8Ag_3Ge_{43}$

table 2. For the large Rb and Ag atoms in $Rb_8Ag_{2.79(4)}Ge_{43.21(4)}$ the Ag/Ge—Ge and Rb—Ge distances are longer than Cu/Ge—Ge and K—Ge distances in $K_{7.69(2)}Cu_{2.94(6)}Ge_{43.06(6)}$.

The crystal structure of $Rb_8Ag_{2.79(4)}Ge_{43.21(4)}$ is shown in figure 2. Pink Rb1 lies in 2*a*, and violet Rb2 at 6*d* sites. Brown Ag1/Ge1 at 6*c* sites, cyan Ge2 at 16*i* and blue Ge3 at 24*k* sites form the fused the violet perpendicular tetrakaidecahedra double chains in the middle of a couple of opposite edges of three directions in the cubic lattice. The yellow pentagonal dodecahedra formed by Ge2 and Ge3 fill the rest vacancies of the corners and body center of the cubic lattice. For $K_{7.69(2)}Cu_{2.94(6)}Ge_{43.06(6)}$ the only difference lies in the K2 split from the center of 6*d* sites to 24 *k* sites with 23.7(1)% occupancy. For simple we give only $Rb_8Ag_{2.79(4)}Ge_{43.21(4)}$ structure. In order to prove if $K_{7.69(2)}Cu_{2.94(6)}Ge_{43.06(6)}$ and $Rb_8Ag_{2.79(4)}Ge_{43.21(4)}$ are semiconductors, theoretical calculations are performed using VASP on ordered $K_8Cu_3Ge_{43}$ and $Rb_8Ag_3Ge_{43}$ models. Calculated band structure and high-symmetry axes of the Brillouin Zone for $K_8Cu_3Ge_{43}$ and $Rb_8Ag_3Ge_{43}$ are shown in figure 3. The abscissa of Figure 3 means the high symmetry directions in Brillouin zone paths (Γ(0, 0, 0)→X(1/2, 0, 0)→M(1/2, 1/2, 0)→Γ(0, 0, 0)→R(1/2, 1/2, 1/2) of the reciprocal lattice. The dashed line corresponds to Fermi energy level. The other multi coloured lines of the figure are electronic energy levels of different bands. The coloured lines are electronic energy bands, which are occupied by electrons below Fermi energy level and are empty above Fermi level. The highest occupied orbit locates at M(1/2, 1/2, 1) direction and the lowest empty orbit lies at X(1/2, 0, 0). The band structure displays a characterized by semiconductor feature with an in indirect band gap of 0.33 and 0.24 eV, respectively. The calculated total and partial density of states are presented in figure 4. The major features can be summarized as follows. The upper VB is mainly derived from Ge 4*p* at the high energy side with partially hybridized Cu *d*/Ag *d* states, while the lower CB is mainly derived from Ge 4*p* at high energy side.

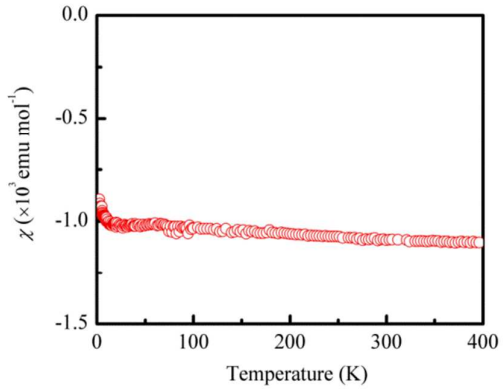

Figure 5. Temperature dependence of susceptibility χ for $K_{7.69(2)}Cu_{2.94(6)}Ge_{43.06(6)}$.

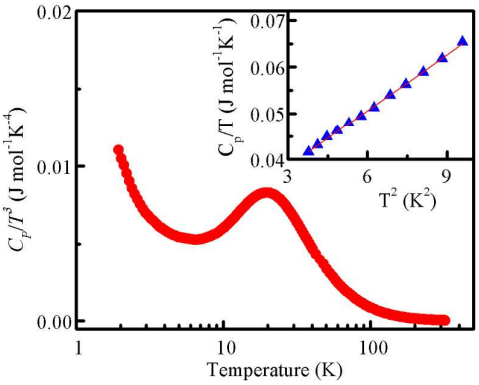

Figure 6. Heat capacity of $K_{7.69(2)}Cu_{2.94(6)}Ge_{43.06(6)}$, plotted as C_p/T^3versus temperature, inset of it is plot as C_p/T versus T^2 with the fitted curve.

The magnetic susceptibility χ versus temperature of $K_{7.69(2)}Cu_{2.94(6)}Ge_{43.06(6)}$ reveals diamagnetic behavior. The susceptibility is $-1.102(1)\times10^{-3}$ emu·mol^{-1} in the field of 7 T at 400 K (Figure 5). Heat capacity can be described by the sum of three contributions: the electronic contribution $C_e = \gamma T$, and the lattice contributions C_l from both the rigid cage forming network and the guest atoms within the cages. The latter two contributions may be described by a Debye term and an Einstein term, respectively. The existence of a low energy Einstein contribution is often motivated by the presence of amaximum in the representation $C_l/T^3 = (C_p - \gamma T)/T^3$ which basically illustrates the deviations from the Debye T^3 law valid in the low T limit. Resorting to the standard description of specific heat, the data can be expressed as $C_p = \gamma T + \beta T^3$. Heat capacity of $K_{7.69(2)}Cu_{2.94(6)}Ge_{43.06(6)}$ plotted as C_p/T^3 versus temperature is shown in Figure 6 and inset of it is plotted as C_p/T versus T^2 with the fitted line. Figure 6 demonstrates that also for $K_{7.69(2)}Cu_{2.94(6)}Ge_{43.06(6)}$ such a maximum at about T = 20 K. The resulting parameters for $K_{7.69(2)}Cu_{2.94(6)}Ge_{43.06(6)}$ from a fit of the data with 1.8 K < T < 3.1 K are γ = 26.6(3) mJ·mol^{-1}·K^{-2} and β = 4.00(4) mJ·mol^{-1}·K^{-4}. The fitted Debye temperature $\Theta_D \approx 297(3)$ K and Einstein temperature $\Theta_E \approx 56.3(1)$ K are obtained.

Experimenal

Synthetic procedures. The target compositions $A_8T_{2.7}Ge_{43.3}$ (A = K, Rb; T = Cu, Ag) are chosen according the Zintl-Klemm rule in order to obtain charge-balanced systems according to $A_8^+T^-_{2.7}Ge^0_{43.3}$. The starting materials are loaded in Ta tubes in molar ratio K/Rb : Cu/Ag : Ge = 8: 2.7: 43.3. The containers are welded in an argon-filled glovebox [$c(O_2)$ and $c(H_2O) \leq 1$ ppm] and sealed in a quartz ampoule in vacuum. After 1 week of heating at 700 °C, the grey products are obtained and washed with distilled water and acetone, then dried at 80 °C for 12h.

Composition. The appropriately prepared metallographic specimens are investigated on a Philips XL 30 scanning electron microscope equipped with LaB_6 cathode. The chemical composition is established with energy dispersive X-ray spectroscopy (EDXS; EDXS Genesis Software V4.61) using Si (Li) detector attacked at the scanning electron microscope. Compositions are calculated from the background-corrected intensities of the X-ray lines K *K*, Rb *L*, Cu *K*, Ag *L* and Ge *K*, which are excited by the electron beam at a 25 kV acceleration voltage. A standardless method with ZAF-matrix corrections is used.

Powder X-ray diffraction The powder XRD patterns are collected by Guinier technique (Huber Image Plate Camera G670, Cu Kα1 radiation, λ = 1.54056 Å, 3.0° < 2ϑ< 100.3°, step width 0.005°). The structures are resolved by powder XRD data by means of least-squares technique using *WinCSD* program[23]. For the structure presentation the program Diamond 3.0 is used.[26]

Theoretical calculation The observed composition is very close to the Zintl count, which may cause the semiconductor-like behaviour. In order to prove this assumption, the first-principles calculations is carried out by means of the density functional theory using the pseudopotential as implemented in the VASP code[27]. The exchange-correlation potential is calculated using the generalized gradient approximation (GGA) as proposed by Perdew Burke Ernzerhof[28]. Throughout the calculations, a 500 eV cutoff in the plane wave expansion and a 6*6*6 Monkhorst-Pack **k** grid are chosen to ensure the calculation with an accuracy of 10^{-5} eV. Furthermore, those calculations are performed using the experimental crystal structure. Because of partial occupancy of K and Cu/Ag and Ge disorders in $K_{7.69(2)}Cu_{2.94(6)}Ge_{43.06(6)}$ and $Rb_8Ag_{2.79(4)}Ge_{43.21(4)}$, we use the integral number ordered $K_8Cu_3Ge_{43}$ and $Rb_8Ag_3Ge_{43}$ lattices with half Cu/Ag and half Ge at 6c sites in order to simplify the calculation.

Physical properties Magnetization is measured from 1.8 to 400 K at 7 T field on a SQUID magnetometer (MPMS, Quantum Design). The heat capacity is determined applying PPMS (Quantum Design, HC option) from 1.8 to 400 K.

Conclusions

$K_{7.69(2)}Cu_{2.94(6)}Ge_{43.06(6)}$ and $Rb_8Ag_{2.83(3)}Ge_{43.17(3)}$ clathrates are synthesized. The lattice parameters and crystal structures are refined by powder XRD data using *WinCSD* package. Theoretical calculation of $K_8Cu_3Ge_{43}$ and $Rb_8Ag_3Ge_{43}$ indicates *p*-type indirect semiconductors with about 0.33 and 0.24 eV band gaps. $K_{7.69(2)}Cu_{2.94(6)}Ge_{43.06(6)}$ is a diamagnetism and has a strong Einstein model in heat capacity. $K_{7.69(2)}Cu_{2.94(6)}Ge_{43.06(6)}$ and $Rb_8Ag_{2.83(3)}Ge_{43.17(3)}$ may be potential *p*-type thermoelectric materials.

Acknowledgements

This work was financially supported by the Strategic Priority Research Program (B) of the Chinese Academy of Sciences (Grants XDB04040200 and XDB04040300), the Natural Science Foundation of China (Grants 91122034, 51125006, 51202279, 61376056, 11204338, 11227902, and 11404359), Science and Technology Commission of Shanghai (Grant 13JC1405700), and Youth Innovation Promotion Association of the Chinese Academy of Sciences (Grant 2015187).

References

1 J. S. Kasper, P. Hagenmuller, M. Pouchard and C. Cros, *Science*, 1965, **150**, 1713.
2 B. Boehme, A. M. Guloy, Z. Tang, W. Schnelle, U. Burkhardt, Baitinger, M. and Yu. Grin, *J. Am. Chem. Soc.* 2007, **129**, 5348.
3 W. Jung, J. Lörincz, R. Ramlau, H. Borrmann, Y. Prots, F. Haarmann, W. Schnelle, U. Burkhardt, M. Baitinger, Yu. Grin, *Angew.Chem.* 2007, **119**, 6846.
4 S. Bobev and S. C. Sevov, *J. Am. Chem. Soc.* 1999, **121**, 3795.
5 A. M. Guloy, R. Ramlau, Z. Tang, W. Schnelle, M. Baitinger, Yu. Grin, *Nature*, 2006, **443**, 320.
6 J. V. Zaikina, K. A. Kovnir, F. Haarmann, W. Schnelle, U. Burkhardt, H. Borrmann, U. Schwarz, Yu. Grin, A. V. Shevelkov, *Chem. Eur. J.* 2008, **14**, 5414.
7 S. Paschen, W. Carrillo-Cabrera, A. Bentien, V. H. Tran, M. Baenitz, Yu. Grin, F. Steglich, *Phys. Rev. B* 2001, **64**, 214404.
8 W. Carrillo-Cabrera, R. Cardoso Gil, V. H. Tran, Yu. Grin, *Z. Kristallogr. NCS*, 2002, **217**, 181.
9 J. T. Zhao and J. D. Corbett, *Inorg. Chem.* 1994, **33**, 5721.
10 M. A. Kirsanova, A. V. Olenev, A. M. Abakumov, M.A. Bykov and A. V. Shevelkov, *Angew. Chem., Int. Ed.* 2011, **50**, 2371.
11 Sloan, E. D., Jr. Clathrate hydrates of natural gases, 2nd ed.; Marcel Dekker Inc.: New York, 1998.
12 G. S. Nolas, J. L. Cohn, G. A. Slack and S. B. Schjuman, *Appl. Phys. Lett.* 1998, **73**, 178.
13 R. Kroener, K. Peters, H. G. von Schnering and R. Nesper, *Z. Kristallogr. NCS*, 1998, **213**, 675.
14 W. Westerhaus and H. U. Schuster, *Z. Kristallogr. B. Anorg. Chemie, Org. Chem.* 1977, **32**, 1365.
15 H. U. Schuster and W. Westerhaus, *Z. Kristallogr. B. Anorg. Chemie, Org. Chem.*, 1975, **30**, 805;
16 S. Sportouch, M. Tillard-Charbonnel and C. Belin, *Z. Kristallogr.*, 1994, **209**, 541.
17 H. G. von Schnering, H. Menke, R. Kroener, E.M. Peters, K. Peters and R. Nesper, *Z. Kristallogr. NCS*, 1998, **213**, 673.
18 R. Kroener, P K. eters, H.G. von Schnering and R. Nesper, *Z. Kristallogr. NCS*, 1998, **213**, 669.
19 H.G. von Schnering, R. Kroener, H. Menke, K. Peters and R. Nesper, *Z. Kristallogr. NCS*, 1998, **213**, 675.
20 A. Kaltzoglou, S. Ponou and T. F. Fässler, *Eur. J. Inorg. Chem*. 2008, 4507.

21 H. Zhang, M. Baitinger, L. Fang, W. Schnelle, H. Borrmann, U. Burkhardt, A. Ormeci, J. T. Zhao, Yu. Grin, *Inorg. Chem*. 2013, **52**, 9720.

22 H. Zhang, H. Borrmann, N. Oeschler, C. Candolfi, W. Schnelle, M. Schmidt, U. Burkhardt, M. Baitinger, J. T. Zhao, Yu. Grin, *Inorg. Chem.* 2011, **50**, 1250-1257.

23 L. G. Akselrud, P. Yu. Zavalii, Yu. Grin, V. K. Pecharsky, B. Baumgartner and E. Wölfel, *Mater. Sci. Forum*, 1993, **133–136**, 335.

24 H.G. von Schnering, H. Menke, *Angew. Chem. Ger. Ed.*, 1972, **84**, 30.

25 N. Jaussaud, P. Toulemonde, M. Pouchard, A. San Miguel, P. Gravereau, S. Pechev, G. Goglio, C. Cros, *Sol. Stat. Sci.,* 2004, **6**, 401.

26 K. Brandenburg, Diamond 3.0; Crystal Impact GbR: Bonn, Germany, 1997–2004.

27 G. Kresse and J. Furthmuller, *Phys. Rev. B* 1996, **54**, 11169.

28 P. Perdew, K. Burke and M. Ernzerhof, *Phys. Rev. Lett*. 1996, **77**, 3865.